

Real-Time Hand Posture Recognition on a Neuromorphic System

Qian Liu, and Steve Furber, *Fellow, IEEE*

Abstract—In order to make an effective, energy-efficient touch-less user interface (UI), we modelled an optimized spiking neural network (SNN) based hand-gesture command identifier on bespoke hardware. Goal 1: prototype a neural gesture recognition system on SpiNNaker. Once the gesture recognition system is functioning effectively the SpiNNaker platform can then be used to explore the optimal spiking neural network size and configuration for the gesture recognition task. Goal 2: evaluate the cost and performance trade-offs in optimizing the number of neural components required to deliver effective gesture recognition.

Keywords—spiking neural network (SNN), convolutional neural network (CNN), posture recognition, neuromorphic system.

I. INTRODUCTION

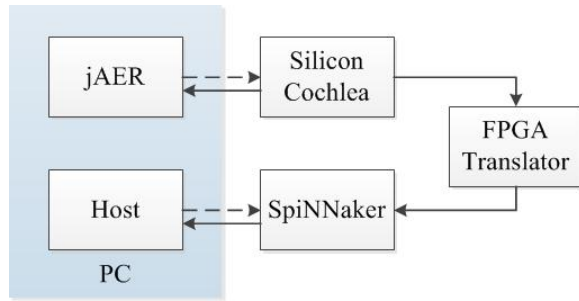
A Pattern or an object in a two-dimensional image can be described with four properties [1]: position, geometry (size, area and shape), color and texture, and trajectory. Appearance-based methods are the most direct approaches to perform pattern recognition. The test image is compared with all the templates to find the best match on one particular or a combination of properties. In terms of classification algorithms, distance measure methods (nearest neighbour, k-means clustering), support vector machine (SVM), multi-layer perceptron (MLP) neural networks and statistical methods, e.g. Gaussian mixture model (GMM) have been applied successfully in visual recognition. Since the 2D projection of an object changes under various illuminations, viewing angles, relative positions and distances (size), it is impossible to represent all appearances of an object in different conditions. Robust matching methods are employed, such as edge matching [2], the divide-and-conquer approach [3], gradient matching [4], etc. Moreover, feature based methods are used to improve reliability, robustness and classification efficiency. Among various feature extraction methods, the scale-invariant feature transform (SIFT) [5] and the sped-up robust features (SURF) [6] methods are well-accepted recently in the field. However, to find a proper feature for a specific object still remains an open question and there is not any process as accurate, general and effective as the brain. Turning to biology for answers is always the way to explore the field of visual pattern recognition. Riesenhuber and Poggio [7] presented a biologically-inspired model following the organization of the visual cortex which has the ability to represent relative position- and scale-invariant features. Integrating a rich set of visual features became available using a feed-forward hierarchical pathway.

More and more attention has been drawn into the investigation of spiking neural networks for vision processing. Pattern information can be encoded in the delays between the pre- and post-synaptic spikes since the spiking neurons are capable of computing radial basis functions (RBFs) [8]. A further study [9] has stated that spatio-temporal information can be also stored in the exact firing time instead of the relative delay. Maass [10] has proved mathematically that: 1) networks of spiking neurons are computationally more powerful than the first and second generation of neural network models; 2) a concrete biologically relevant function can be computed by a single spiking neuron, replacing hundreds of hidden units in a sigmoidal neural net; 3) any function that can be computed by a small sigmoidal neural net can also be computed by a small network of spiking neurons. Applications of SNN-based vision processing have been successfully carried out. A two-layered SNN has been trained using spike time dependent plasticity (STDP) and employed for a character recognition task [11]. Lee and co-authors [12] have implemented the direction selective filters in real time using spiking neurons. The direction selective filters here are considered as a layer of convolution module in the model of so called convolution neural network [13]. Different features, such as Gabor filter features (scale, orientation and frequency) and shape can be modelled as layers of feature maps. Rank order coding, as an alternative to conventional rate-based coding, treats the first spike the most important and has well applied to an orientation detection training process [14]. Nengo [15] is a graphical and scripting based software package for simulating large-scale neural systems and has been used to build the world's largest functional brain model, Spaun [16]. An FPGA implementation of a Nengo model for digit recognition has been reported [17]. Deep Belief Networks (DBNs), the 4th generation of artificial neural network, has shown a strong ability in solving classification problems. A recent study [18] has resoundingly mapped an offline-trained DBN onto an efficient event-driven spiking neural network for a digit recognition task. Hand segmentation and feature extraction usually takes the colour into account and involves wavelets, e.g. using a Kalman filter. Thus, shape-only recognition of the hand posture will be a challenge. In the terms of gesture recognition, the hidden Markov model (HMM) has shown its ability to recognize dynamic gestures [19]. However, with their instinctive temporal processing, SNNs have the potential to deliver dynamic gesture recognition.

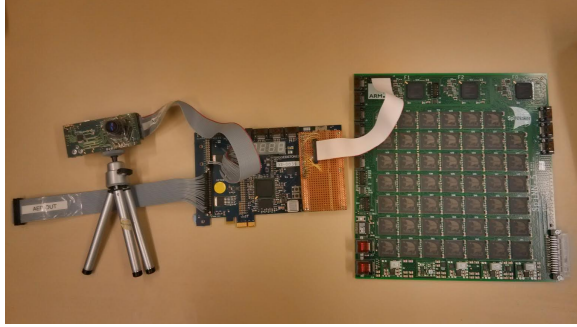
II. NEUROMORPHIC PLATFORM

This section presents some details of the two hardware components, the Address-Event Representation (AER) silicon

The authors are with the School of Computer Science, University of Manchester, Manchester M13 9PL, U.K. (e-mail:liuq@cs.man.ac.uk; steve.furber@manchester.ac.uk).



(a) Outline of the platform



(b) Picture of the hardware platform

Fig. 1: System overview of the posture recognition platform. The silicon retina connects to the SpiNNaker system through an FPGA board. Spikes from the retina are streamed to the SpiNNaker system through this Spartan-6 FPGA board. The jAER software configures the retina and displays its outgoing spikes through the USB connection. The host sets up the runtime parameters off-line and downloads the network model to the SpiNNaker system.

retina [20] and the SpiNNaker system [21] which is a massive parallel computing platform aimed at real-time simulation of spiking neural networks (SNNs). Figure 1 shows the combined hand posture recognition system; the AEREAR2 silicon retina connected to the SpiNNaker 48-node board via a Spartan 6 FPGA board [22]. The jAER [23] event-based processing software¹ running on the PC configures the retina and displays the output spikes through a USB link. The host communicates to the SpiNNaker board via Ethernet to set up its runtime parameters and to download the neural network model off-line and uses a visualiser [24] to show the spiking activities in real-time.

A. Silicon Retina

The visual front-end is constituted by a Dynamic Video Sensor (DVS) silicon retina, an asynchronous sensor which provides spike events encoding the address of pixels undergoing a contrast change[4]. This approach lies in opposition to the more traditional method of sending entire frames to provide fast (3 μ s latency) data-driven contrast detection at a wide range of illuminations. The sensor is capable of transmitting from 1 Keps to 20 Meps (events per second).

¹<http://sourceforge.net/p/jaer/wiki/Home/>

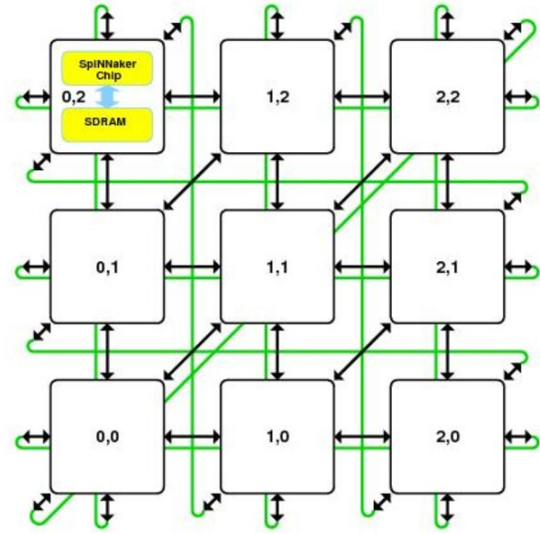


Fig. 2: System diagram

B. SpiNNaker System

The SpiNNaker project's architecture mimics the human brain's biological structure and functionality. This offers the possibility of utilizing massive parallelism and redundancy to provide resilience in an environment of unreliability and failure of individual components.

In the human brain, communication between its computing elements, or neurons, is achieved by the transmission of electrical "spikes" along connecting axons. The biological processing of the neuron can be modelled by a digital processor and the axon connectivity can be represented by messages, or information packets, transmitted between a large number of processors which emulate the parallel operation of the billions of neurons comprising the brain.

The engineering of the SpiNNaker concept is illustrated in the Figure 2 where the hierarchy of components can be identified. Each element of the toroidal interconnection mesh is a multi-core processor known as the "SpiNNaker Chip" comprising 18 processing cores. Each core is a complete processing sub-system with local memory and a DMA capability. It is connected to its local peers via a Network-on-Chip (NoC) which provides local high bandwidth communication and to other SpiNNaker chips via links between SpiNNaker chips. In this way the massive parallelism extending to thousands or millions of processors is possible.

The knowledge content and learning ability of the brain is embodied in its evolvable interconnection pattern; this routes a spike generated by one neuron to others which are interconnected with it by axons and these interconnections are modified and extended as a result of the learning and processes.

In SpiNNaker a packet Router within each multi-core processor controls the neural interconnection. Each transmitted packet representing a spike contains information which identifies its source neuron; this is used by a multi-core processor's Router to identify whether this packet should be routed to one

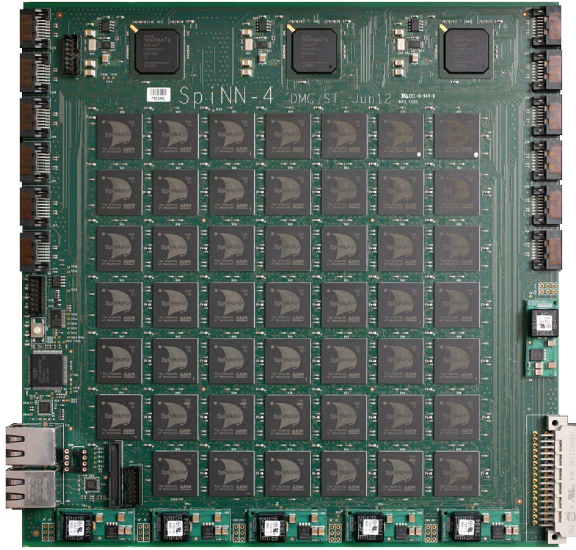


Fig. 3: 103 Machine PCB

of its contained application processors to respond, or should be routed on to one of the six adjacent multi-core processors connected to it as part of the overall SpiNNaker network.

The 103 machine is the 48-node board, see Figure 3, and has 864 ARM processor cores, typically deployed as 768 application cores, 48 Monitor Processors and 48 spare cores. The 103 machine requires a 12V 6A supply. The control interface is two 100Mbps Ethernet connections, one for the Board Management Processor and the second for the SpiNNaker array. There are options to use the nine on-board 3.1Gbps high-speed serial interfaces (using SATA cables, but not necessarily the SATA protocol) for I/O; this will require suitable configuration of the on-board FPGAs that provide the high-speed serial interface support. 103 boards can be connected together to form larger systems using the high-speed serial interfaces.

C. Interfacing AER Sensors

Spikes from the silicon retina are injected to SpiNNaker through one of the 6 bi-directional on-board links by a SPARTAN-6 FPGA board that translates them into a SpiNNaker compatible AER format². From the software point of view, interfacing the silicon retina can be done using pyNN. The user sets a Spike Source population that resides on a virtual SpiNNaker chip, to which an AER sensor's spikes are directed, thus abstracting away the hardware details from the users[22].

III. CONVOLUTIONAL NEURAL NETWORKS

The convolutional neural network (CNN) is well-known as an example of a biologically-inspired model. The repeated convolutional kernels are overlapped in the receptive fields of the input neurons. Figure 4 shows a typical convolutional connection between two layers of neurons.

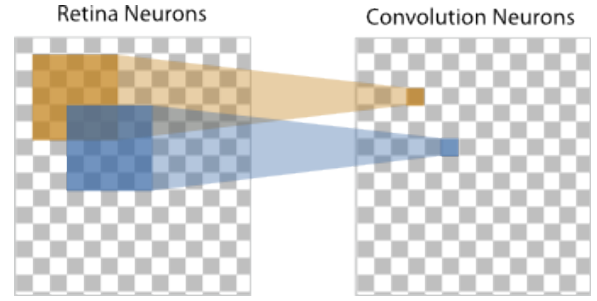


Fig. 4: Each individual convolution neuron connects to its respective field using the same kernel.

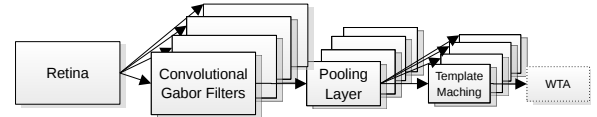


Fig. 5: The convolutional neural network model with manually selected templates.

A. Model Description

There are two CNNs proposed to accomplish the posture recognition task. A straight forward method of template matching was employed at first, and then a multi-layer perceptrons (MLP) was trained to improve the recognition performance.

1) *Manual Feature Extraction Model*: Shown in Figure 5 the first two layers are the input layer and the convolution layer, where the kernels are Gabor filters responding to four orientations. The third layer is the pooling layer where the size of the populations shrinks. This down-sampling enables robust classification due to its tolerance to variations in the precise shape of the input. The fourth layer is another convolution layer where the output from the pooling layer is convolved with the templates. Each template is a frame (one frame consists of 30ms of spiking activity) of output spikes from the pooling layer. The Gabor filter is well-known as a linear filter for edge detection in image processing. A Gabor filter is a 2D convolution of a Gaussian kernel function and a sinusoidal plane wave; see Equation 1. θ represents the orientation of the filter, λ is the wavelength of the sine wave, and σ is the standard deviation of the Gaussian envelope. The frequency and orientation features are similar to the responses of V1 neurons in the human visual system. Only the real parts of the Gabor filters (see Figure 6) are used as the convolutional kernels to configure the weights between the input layer and the Gabor filter layer.

²AppNote 8 - Interfacing AER devices to SpiNNaker using an FPGA.

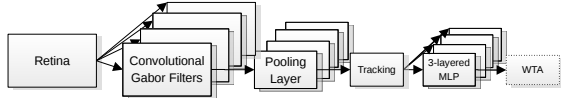


Fig. 8: The combined convolutional model with trained MLP neurons.

$$\begin{aligned}
 \text{RealParts} &= \exp\left(\frac{-x'^2 + y'^2}{2\sigma^2}\right) \cos\left(2\pi\frac{x'}{\lambda}\right) \\
 \text{ImaginaryParts} &= \exp\left(\frac{-x'^2 + y'^2}{2\sigma^2}\right) \sin\left(2\pi\frac{x'}{\lambda}\right)
 \end{aligned} \tag{1}$$

where :

$$\begin{aligned}
 x' &= x \cos(\theta) + y \sin(\theta) \\
 y' &= -x \sin(\theta) + y \cos(\theta)
 \end{aligned}$$

The templates (see Figure 7) are manually selected from the output of the pooling layer in the framed Matlab simulation. The output score of a convolution neuron is higher when its receptive field matches a certain template more. There are five populations of template matching neurons for five postures in our system. The activity of the template matching populations indicates naturally the position of the postures.

2) *Combined Convolution Network*: Inspired by the research of Lecun [25] and etc., we designed a combined network model with MLP and the convolutional network (Figure 8). Thanks to the help of tracking, only the most active region in the pooling layer is forwarded to the next layer. A trained static 3-layered MLP is attached to classify the posture.

Since the size of the input image of the MLP training is fixed and the position is centered, tracking plays a very important role to spot the valid region. Tracking is naturally embedded in the pooling layer of the convolutional network, for the active neurons directly point out the lively receptive field. However, to extract only the active region to the next layer is still need to investigate.

B. Training and Testing

Training is missing here.

In order to evaluate the cost and performance trade-offs in optimizing the number of neural components, both the convolutional models described above were tested at different sizes. Five videos of every posture were captured from the silicon retina in address-event representation (AER [26]) format. All the postures are of similar size and moving clock-wise in front of the retina. The videos are cut into frames (30 ms per frame) and push forward into the convolutional networks. The configurations of the networks are listed in Table I (Model 1: template matching; Model 2: trained MLP). The integration layer is not necessary in a convolutional network, it is used here to fit the template matching and decrease the number of synaptic connections.

TABLE I: Sizes of the convolutional neural networks.

(a) Model 1: Template matching

	Full Resolution		Sub-sampled Resolution	
	Neuron Number	Connections per Neuron	Neuron Number	Connections per Neuron
Retinal Input	128 × 128	1	32 × 32	4 × 4
Gabor Filter	112×112×4	17 × 17	28×28×4	5 × 5
Pooling Layer	36×36×4	5 × 5	null	null
Integration Layer	36 × 36	4	28 × 28	4
Template Matching	16×16×5	21 × 21	14×14×5	15 × 15
Total	74320	15216512	5925	318420

(b) Model 2: Trained MLP network layers after tracking

	Full Resolution		Sub-sampled Resolution	
	Neuron Number	Connections per Neuron	Neuron Number	Connections per Neuron
Tracked Input	21 × 21	null	15 × 15	null
Hidden Layer	10	21×21×10	10	15×15×10
Recognition Layer	5	5×10	5	5×10
Total	456	4460	240	2300

C. Experiment Results

In Figure 9 the first two plots refer to Model 1, using template matching. Each colour represents one of the recognition populations. Each point in the plot is the highest neuronal response in the recognition population during the time of one frame (30 ms). The neuronal response, the spiking rate, is normalized to [-1, 1]. It can be seen that the higher resolution input makes the boundaries between the classes clearer. On the other hand, recognition only happens when the test image and template are similar enough. The templates are only selected from the frames where the gestures are moving towards the right, and the gestures are moving clockwise in the videos. Thus, all the peaks in plot 1 signify that the direction of the gestures movement is right. It is notable that the higher resolution causes the recogniser to be more sensitive to the differences between the test data and the template, while the smaller neural network can recognize more generalized patterns. Therefore, a threshold is required to differentiate between data that is close enough and that which is not. Since the gestures are moving in four different directions during the clockwise movement, a rejection rate of 75% is to be expected. The latter two plots refer to Model 2. The three-layer MLP network significantly improves the recognition rate and can generalize the pattern. There is no rejection rate for Model 2. The detailed results are listed in Table II. The correct recognition rate is calculated from the non-rejected frames. The lower resolution of the 32×32 retina input is adequate for this gesture recognition task. The smaller network uses only 1/10 the number of neurons and 1/50 the number of synaptic connections compared to the full resolution network, while

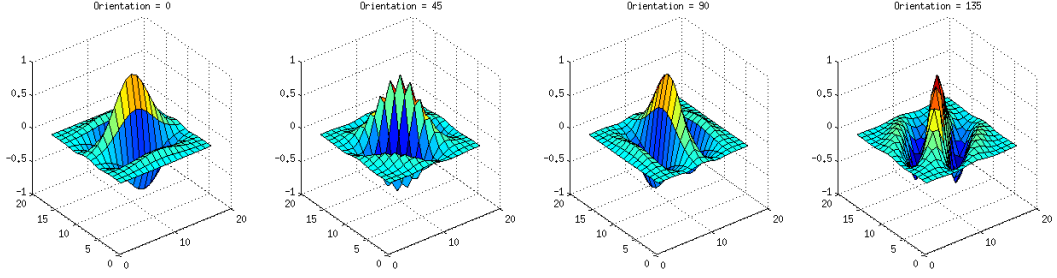


Fig. 6: Real parts of the Gabor filters oriented to four directions.

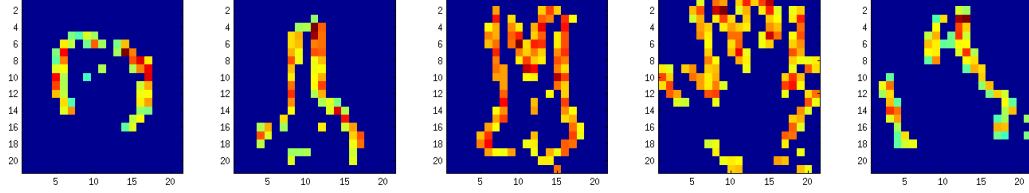


Fig. 7: Templates of the Five Postures.

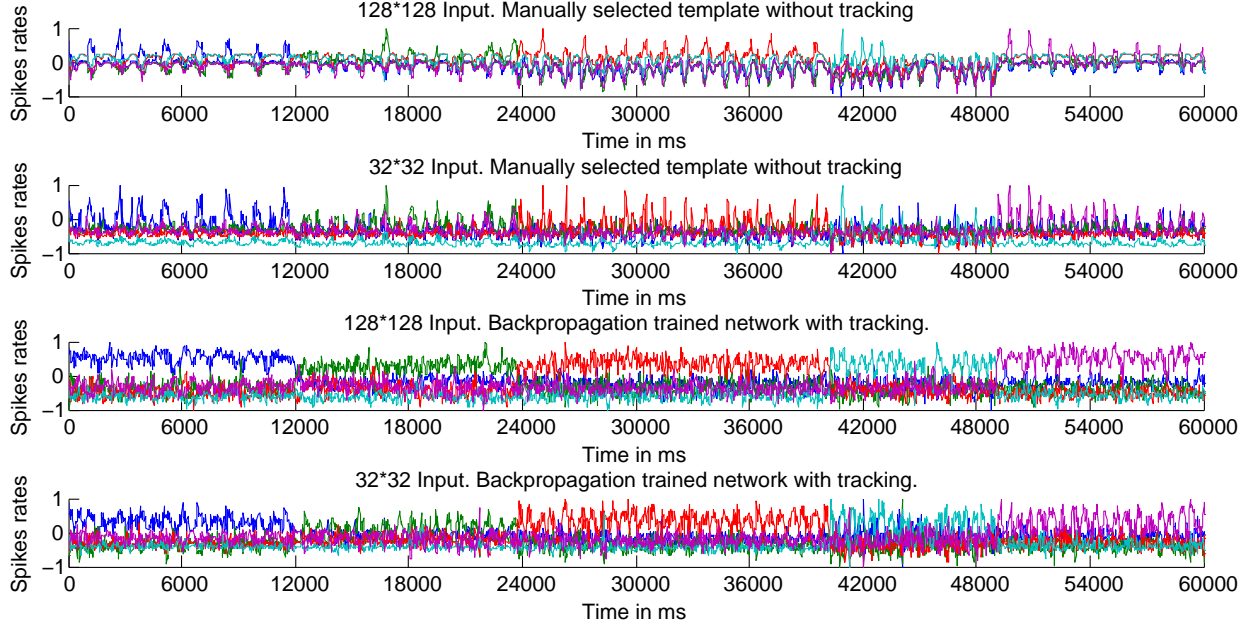


Fig. 9: Neural responses with time to the same recorded postures.

the recognition rate drops only around 10% with Model 1 and 15% with Model 2.

IV. REAL-TIME RECOGNITION ON SPINNAKER

A. Moving from Rate-based Artificial Neurons to Spiking Neurons

It remains a challenge to transfer a traditional artificial neural networks into the spiking ones. There are attempts [27] [28] to estimate the output firing rate of the Leaky integrate-and-fire (LIF) neurons (Equation 2) under certain conditions.

$$\frac{dV(t)}{dt} = -\frac{V(t) - V_{rest}}{\tau_m} + \frac{I(t)}{C_m} \quad (2)$$

TABLE II: Recognition results

		Model 1		Model 2	
		High Resolution	Low Resolution	High Resolution	Low Resolution
Fist	Correct	99.11%	99.23%	96.24%	84.21%
	Reject	71.93%	67.42%	Null	Null
One Finger (392 Frames)	Correct	92.98%	80.00%	94.39%	71.69%
	Reject	70.92%	75.77%	Null	Null
Victory Sign (551 Frames)	Correct	96.56%	93.07%	95.64%	87.66%
	Reject	73.68%	81.67%	Null	Null
Full Hand (293 Frames)	Correct	95.65%	72.41%	93.52%	72.01%
	Reject	92.15%	90.10%	Null	Null
Thumb up (391 Frames)	Correct	89.61%	84.44%	96.68%	74.68%
	Reject	80.31%	76.98%	Null	Null

The membrane potential V evolves with the input current I starting from the resting membrane potential V_{rest} , where the membrane time constant $\tau_m = R_m C_m$, and R_m stands for the membrane resistance and C_m the membrane capacitance.

Given a fixed constant current injection I , the response function, firing rate, of the LIF neuron is

$$\lambda_{out} = \left[t_{ref} - \tau_m \ln \left(1 - \frac{V_{th} - V_{rest}}{IR_m} \right) \right]^{-1} \quad (3)$$

when $IR_m > V_{th} - V_{rest}$, otherwise the membrane potential cannot reach the threshold V_{th} and the output firing rate is zero. The absolute refractory period t_{ref} is included, for all the input during the period is invalid. In a more realistic scenario, the post-synaptic potentials (PSPs) are triggered by the spikes generated from the neuron's pre-synaptic neurons other than a constant current. Assume that the synaptic inputs are Poisson spike trains, the membrane potential of the LIF neuron is concerned as a diffusion process. Equation 2 can be modelled as a stochastic differential equation referring to Ornstein-Uhlenbeck process,

$$\tau_m \frac{dV(t)}{dt} = -[V(t) - V_{rest}] + \mu + \sigma \sqrt{2\tau_m} \xi(t) \quad (4)$$

where

$$\begin{aligned} \mu &= \tau_m (\mathbf{w}_E \cdot \lambda_E - \mathbf{w}_I \cdot \lambda_I) \\ \sigma^2 &= \frac{\tau_m}{2} (\mathbf{w}_E^2 \cdot \lambda_E + \mathbf{w}_I^2 \cdot \lambda_I) \end{aligned} \quad (5)$$

are the conditional mean and variance of the membrane potential. The delta-correlated process $\xi(t)$ is a Gaussian white noise with zero mean, $\mathbf{w}_I, \mathbf{w}_I$ stand for the weight vectors of the excitatory and the inhibitory synapses, and λ represents the vector of the input firing rate. The response function of the LIF neuron with Poisson input spike trains is given by Siegert function [29],

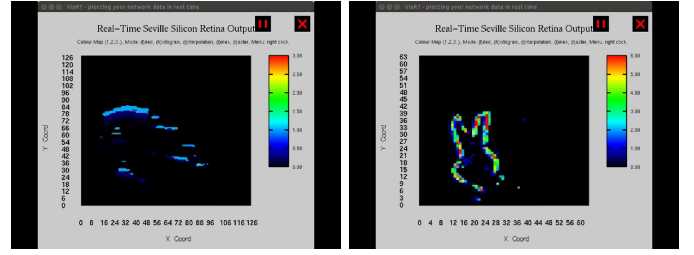
$$\lambda_{out} = \left(\tau_{ref} + \frac{\tau_Q}{\sigma_Q} \sqrt{\frac{\pi}{2}} \int_{V_{rest}}^{V_{th}} du \exp \left(\frac{u - \mu_Q}{\sqrt{2}\sigma_Q} \right)^2 \cdot \left[1 + \operatorname{erf} \left(\frac{u - \mu_Q}{\sqrt{2}\sigma_Q} \right) \right] \right)^{-1} \quad (6)$$

where τ_Q, μ_Q, σ_Q are identified to τ_m, μ, σ in Equation 5, and erf is the error function.

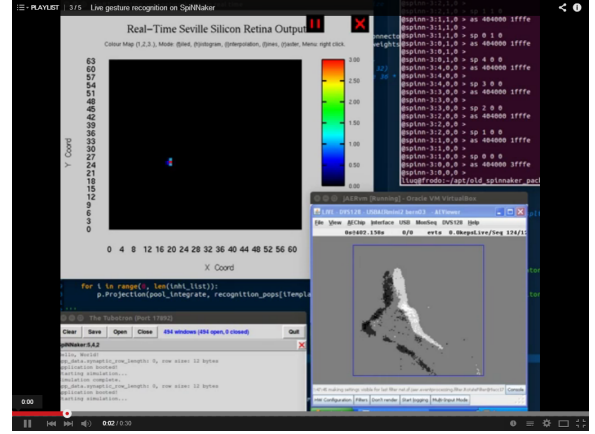
Still there are some limitations on the response function. For the diffusion process, only small amplitude(weight) of the PSPs generated by a large amount of input spikes(high spiking rate) works under this circumstances; plus, the delta function is required (the synaptic time constant is considered to be zero). Thus only a rough approximation of the output spike rate has been taken out. Secondly, given the input spike rates of the pre-synaptic neurons, the parameters of the LIF neuron and the output spiking rate, how to tune the every corresponding synaptic weight remains a hard task.

B. Live Recognition

We implemented the prototype of the neural gesture recognition system on SpiNNaker. The input retina layer consists of 128×128 neurons; each Gabor filter has 112×112 valid



(a) Neural responses of the Gabor (b) Neural responses of the integration layer orienting to the horizontal direction



(c) Snapshot of the neuron responses of the template matching layer

Fig. 10: Snapshots of the real-time gesture recognition system on SpiNNaker.

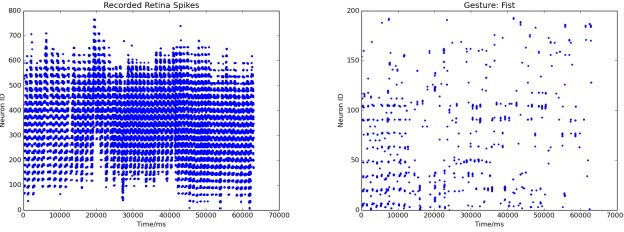
neurons, since the kernel size is 17×17 ; each pooling layer is as big as 36×36 , convolving with five template kernels (21×21); thus, the recognition populations are 16×16 neurons each. Altogether 74320 neurons and 15216512 synapses, see Table Ia, use up to 19 chips (290 cores) on a 48-node board. Regarding the lower resolution of 32×32 retinal input, see Table Ib, the network consists of 5925 neurons and 318420 synapses taking up only two chips (31 cores) of the board.

Figure 10 shows snapshots of the real time gesture recognition system. Figure 10a is a snapshot of the Gabor filter layer, where Figure 10b shows the integration of all the pooled populations, and the active neurons in the visualizer in Figure 10c are pointing out the position of the recognized pattern (One finger). All the videos can be found on Youtube³.

C. Recognition of Recorded Data

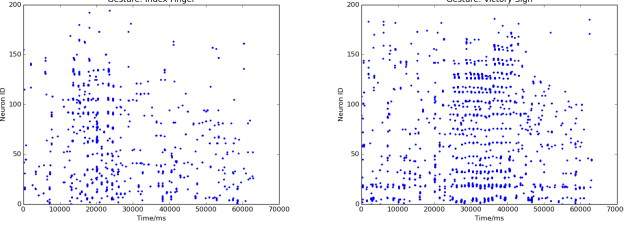
To compare with the results of the experiments taken out in Section III-C with Matlab, the same recorded retinal data is conducted to SpiNNaker. The recorded data is presented as Spike Source Array in the system with 128×128 input, see Figure 13a, while the data is forwarded to a sub-sampling layer of 32×32 resolution, see Figure 11a, in the system of the smaller network. The output spikes generated from the

³<http://youtu.be/PvJy6RKAJhw?list=PLxZ1W-Upr3eoQuLxq87qpUL-CwSptEBJ>,
<http://youtu.be/FZJshPCJ1pg?list=PLxZ1W-Upr3eoQuLxq87qpUL-CwSptEBJ>,
<http://youtu.be/yxN90aGGKvg?list=PLxZ1W-Upr3eoQuLxq87qpUL-CwSptEBJ>



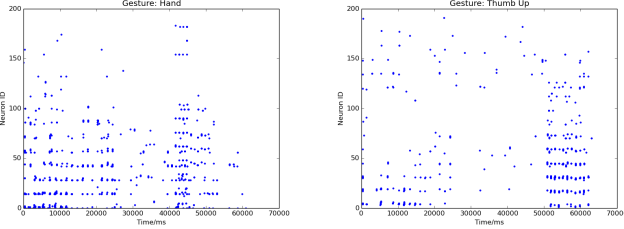
(a) Retinal input population

(b) Template matching population, 'Fist'



(c) Template matching population, 'Single Finger'

(d) Template matching population, 'Victory Sign'



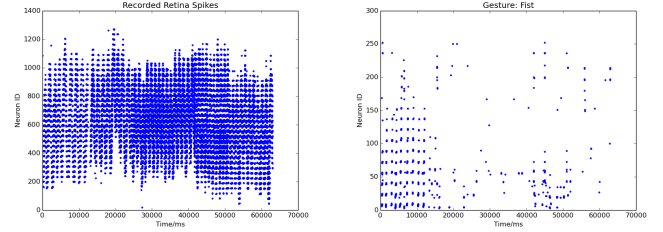
(e) Template matching population, 'Full Hand'

(f) Template matching population, 'Thumb Up'

Fig. 11: Spikes captured during the live recognition of the recorded retinal input with the resolution of 32×32 .

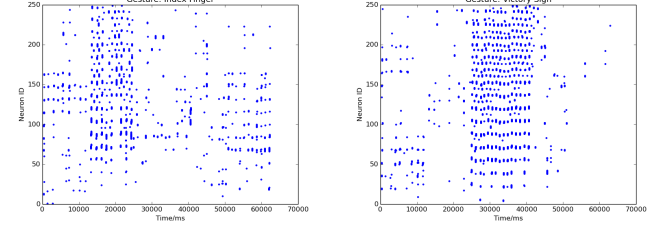
recognition populations with time are shown in Figure 13 and 11 respectively for both the full resolution and the lower systems. More spikes generated during the period when the preferred input gesture is shown.

Correspondingly, the spiking rates of each recognition population is sampled into frames (Figure 12) to make a comparison with the Matlab simulation. Each colour represents one recognition population, and the spike activity goes higher when the input gesture matches the template. Firstly, the spike rates are sampled into 30 ms frames which is in accordance with the Matlab experiments. In the Matlab simulation, the templates are trained with cut frames and so as the test images are also fixed to the same length frames. Otherwise, the recogniser will not work properly because of the replications of the moving posture. On the contrast, the spiking rates can be sampled to various lengths of frames. Thus, the other two plots in the figure illustrate the classification in a wider window, 300 ms . From Table III, the recognition rates as well as the rejection rates are quantified in percentage. Regarding the latency between the retinal input and the recognition, we compared the spiking peak of the Matlab simulation and the real-time SpiNNaker test. The overall latency is about 1150 ms from a posture is shown to its recognition.



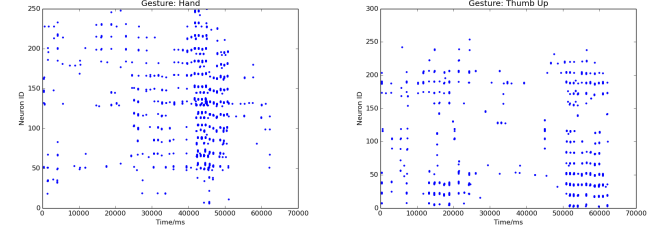
(a) Retinal input population

(b) Template matching population, 'Fist'



(c) Template matching population, 'Single Finger'

(d) Template matching population, 'Victory Sign'



(e) Template matching population, 'Full Hand'

(f) Template matching population, 'Thumb Up'

Fig. 13: Spikes captured during the live recognition of the recorded retinal input with the resolution of 128×128 .

TABLE III: Recognition results on SpiNNaker in real time

		30 ms per frame		300 ms per frame	
		High Resolution	Low Resolution	High Resolution	Low Resolution
Fist	Correct	91.78%	78.02%	100%	92.31%
	Reject	82.78%	78.54%	70.73%	68.29%
One Finger	Correct	78.25%	78.25%	88.24%	72.22%
	Reject	80.46%	73.56%	57.50%	55.00%
Victory Sign	Correct	96.48%	86.27%	95.00%	92.50%
	Reject	64.46%	72.68%	28.57%	28.57%
Full Hand	Correct	85.29%	60.78%	90.00%	75.00%
	Reject	67.31%	83.65%	35.48%	61.29%
Thumb up	Correct	84.09%	88.10%	91.67%	100%
	Reject	87.54%	73.81%	66.67%	66.67%

V. CONCLUSION AND FUTURE WORK

The future work will include more collaboration with biology and work with neuroscientist on vision systems, especially on the orientation detection region. To equip the system with tracking is another important job where the recognition performance will be increased and the short-term memory of a gesture route can be stored. Using the idea of HMMs to spiking neural networks may be a good approach.

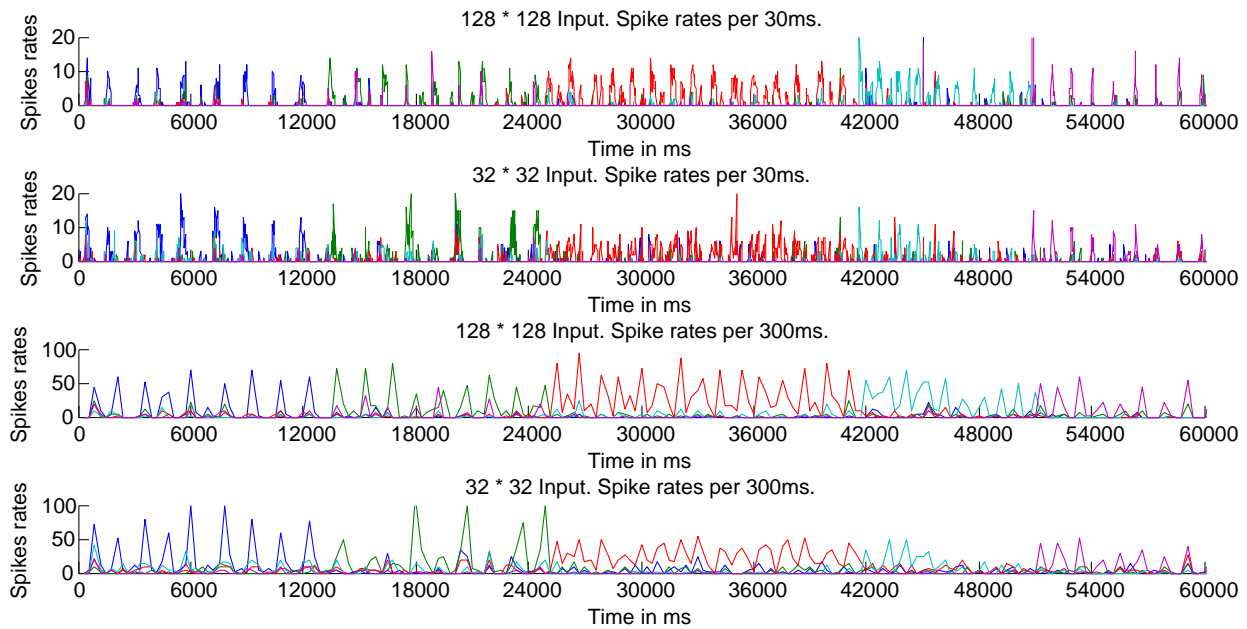


Fig. 12: Real time neural responses on SpiNNaker with time to the same recorded postures.

VI. ACKNOWLEDGEMENT

This research was supported by Samsung under their GRO programme. The authors appreciate the collaboration with Prof. Bernabé Linares-Barranco and Luis Camunas-Mesa on the silicon retina. The authors would like to thank the meaningful discussions with Evangelos Stomatias, Patrick Camilleri and Michael Hopkins.

REFERENCES

- [1] S. G. Wysocki, L. Benuskova, and N. Kasabov, "Fast and adaptive network of spiking neurons for multi-view visual pattern recognition," *Neurocomputing*, vol. 71, no. 13, pp. 2563–2575, 2008.
- [2] J. Canny, "A computational approach to edge detection," *Pattern Analysis and Machine Intelligence, IEEE Transactions on*, no. 6, pp. 679–698, 1986.
- [3] Ö. Toygar and A. Acan, "Multiple classifier implementation of a divide-and-conquer approach using appearance-based statistical methods for face recognition," *Pattern Recognition Letters*, vol. 25, no. 12, pp. 1421–1430, 2004.
- [4] S.-D. Wei and S.-H. Lai, "Robust and efficient image alignment based on relative gradient matching," *Image Processing, IEEE Transactions on*, vol. 15, no. 10, pp. 2936–2943, 2006.
- [5] D. G. Lowe, "Distinctive image features from scale-invariant keypoints," *International journal of computer vision*, vol. 60, no. 2, pp. 91–110, 2004.
- [6] H. Bay, A. Ess, T. Tuytelaars, and L. Van Gool, "Speeded-up robust features (surf)," *Computer vision and image understanding*, vol. 110, no. 3, pp. 346–359, 2008.
- [7] M. Riesenhuber and T. Poggio, "Hierarchical models of object recognition in cortex," *Nature neuroscience*, vol. 2, no. 11, pp. 1019–1025, 1999.
- [8] J. J. Hopfield, "Pattern recognition computation using action potential timing for stimulus representation," *Nature*, vol. 376, no. 6535, pp. 33–36, 1995.
- [9] T. Natschläger and B. Ruf, "Spatial and temporal pattern analysis via spiking neurons," *Network: Computation in Neural Systems*, vol. 9, no. 3, pp. 319–332, 1998.
- [10] W. Maass, "Networks of spiking neurons: the third generation of neural network models," *Neural networks*, vol. 10, no. 9, pp. 1659–1671, 1997.
- [11] A. Gupta and L. N. Long, "Character recognition using spiking neural networks," in *Neural Networks, 2007. IJCNN 2007. International Joint Conference on*, pp. 53–58, IEEE, 2007.
- [12] J. H. Lee, P. Park, C.-W. Shin, H. Ryu, B. C. Kang, and T. Delbruck, "Touchless hand gesture ui with instantaneous responses," in *Image Processing (ICIP), 2012 19th IEEE International Conference on*, pp. 1957–1960, Sept 2012.
- [13] L. Camunas-Mesa, C. Zamarreno-Ramos, A. Linares-Barranco, A. J. Acosta-Jimenez, T. Serrano-Gotarredona, and B. Linares-Barranco, "An event-driven multi-kernel convolution processor module for event-driven vision sensors," *Solid-State Circuits, IEEE Journal of*, vol. 47, no. 2, pp. 504–517, 2012.
- [14] A. Delorme, L. Perrinet, and S. J. Thorpe, "Networks of integrate-and-fire neurons using rank order coding b: spike timing dependent plasticity and emergence of orientation selectivity," *Neurocomputing*, vol. 38, pp. 539–545, 2001.
- [15] C. Eliasmith and T. C. Stewart, "Nengo and the neural engineering framework: connecting cognitive theory to neuroscience," in *Proceedings of the 33rd annual meeting of the cognitive science society*, pp. 1–2, 2011.
- [16] C. Eliasmith, T. C. Stewart, X. Choo, T. Bekolay, T. DeWolf, Y. Tang, and D. Rasmussen, "A large-scale model of the functioning brain," *science*, vol. 338, no. 6111, pp. 1202–1205, 2012.
- [17] M. Naylor, P. J. Fox, A. T. Markettos, and S. W. Moore, "Managing the fpga memory wall: Custom computing or vector processing?," in *Field Programmable Logic and Applications (FPL), 2013 23rd International Conference on*, pp. 1–6, IEEE, 2013.
- [18] P. O'Connor, D. Neil, S.-C. Liu, T. Delbruck, and M. Pfeiffer, "Real-time classification and sensor fusion with a spiking deep belief network," *Frontiers in neuroscience*, vol. 7, 2013.
- [19] M. Elmezain, A. Al-Hamadi, J. Appenrodt, and B. Michaelis, "A hidden markov model-based isolated and meaningful hand gesture recognition," *International Journal of Electrical, Computer, and Systems Engineering*, vol. 3, no. 3, pp. 156–163, 2009.
- [20] J. A. Leñero-Bardallo, T. Serrano-Gotarredona, and B. Linares-Barranco, "A 3.6 s latency asynchronous frame-free event-driven dynamic-vision-sensor," *Solid-State Circuits, IEEE Journal of*, vol. 46, no. 6, pp. 1443–1455, 2011.
- [21] S. B. Furber, F. Galluppi, S. Temple, and L. A. Plana, "The spinnaker project," 2014.
- [22] F. Galluppi, K. Brohan, S. Davidson, T. Serrano-Gotarredona, J.-A. P. Carrasco, B. Linares-Barranco, and S. Furber, "A real-time, event-driven neuromorphic system for goal-directed attentional selection," in *Neural Information Processing*, pp. 226–233, Springer, 2012.
- [23] T. Delbruck, "Frame-free dynamic digital vision," in *Proceedings of Intl. Symp. on Secure-Life Electronics, Advanced Electronics for Quality Life and Society*, pp. 21–26, 2008.
- [24] C. Patterson, F. Galluppi, A. Rast, and S. Furber, "Visualising large-scale

neural network models in real-time,” in *Neural Networks (IJCNN), The 2012 International Joint Conference on*, pp. 1–8, 2012.

- [25] Y. LeCun, L. Bottou, Y. Bengio, and P. Haffner, “Gradient-based learning applied to document recognition,” *Proceedings of the IEEE*, vol. 86, no. 11, pp. 2278–2324, 1998.
- [26] J. Lazzaro and J. Wawrzynek, “A multi-sender asynchronous extension to the aer protocol,” in *Advanced Research in VLSI, Conference on*, pp. 158–158, IEEE Computer Society, 1995.
- [27] G. La Camera, M. Giugliano, W. Senn, and S. Fusi, “The response of cortical neurons to in vivo-like input current: theory and experiment,” *Biological cybernetics*, vol. 99, no. 4-5, pp. 279–301, 2008.
- [28] A. N. Burkitt, “A review of the integrate-and-fire neuron model: I. homogeneous synaptic input,” *Biological cybernetics*, vol. 95, no. 1, pp. 1–19, 2006.
- [29] A. J. Siegert, “On the first passage time probability problem,” *Physical Review*, vol. 81, no. 4, p. 617, 1951.

Qian Liu Biography text here.

PLACE
PHOTO
HERE

Steve Furber Biography text here.

PLACE
PHOTO
HERE